Water Air Soil Pollut (2007) 186:273–288
DOI 10.1007/s11270-007-9483-0

Nutrient Input Through Occult and Wet Deposition into a Subtropical Montane Cloud Forest

E. Beiderwieden · A. Schmidt · Y.-J. Hsia · S.-C. Chang · T. Wrzesinsky · O. Klemm

Received: 16 April 2007 / Accepted: 28 July 2007 / Published online: 6 September 2007

Abstract Chemical composition of fog and rain water was studied during a 47-day experimental period. The differences between the fog and rain water were found to be significantly for most analyzed ions. H^+, NH_4^+, NO_3^-, and SO_4^{2-} made up 85% of the total median ion concentration in fog and 84% in rain water. The total mean equivalent concentration was 15 times higher in the fog than in the rain water. The fog water samples were classified according to their air mass history. The analysis of the 120 h backward trajectory led to the identification of three advection regimes. Significant differences of ion concentrations between the respective classes were found. Air masses of class I travelled exclusively over the Pacific Ocean, class II were carried over the Philippines, and class III were advected from mainland China. The turbulent fog water deposition was determined by the means of the eddy covariance method. The total (turbulent plus gravitational) fog water fluxes ranged between +31.7 mg m^{-2} s^{-1} and −56.6 mg m^{-2} s^{-1}. Fog water droplets with mean diameters between 15 μm and 25 μm contributed most to the liquid water flux. The sample based nutrient input was calculated on the basis of the occult and wet deposition, and the concentrations of the simultaneously collected fog and rainwater samples, respectively. The nutrient input through wet deposition was about 13 times higher than through occult deposition.

Keywords Eddy covariance · Turbulent fog water fluxes · Atmospheric deposition · Trajectories · Artificial neural network · Cypress forest

E. Beiderwieden (✉) · A. Schmidt · T. Wrzesinsky · O. Klemm
Institute for Landscape Ecology, University of Münster,
Robert-Koch-Str. 26,
48149 Münster, Germany
e-mail: beiderwieden@uni-muenster.de

Y.-J. Hsia · S.-C. Chang
Institute of Natural Resources,
National Dong Hwa University,
974 Hualien, Taiwan

1 Introduction

Montane cloud forests are defined as forests that are frequently covered in cloud or mist (Stadtmüller 1987; Hamilton et al. 1995). In the tropics, they typically occur between 1,200 m and 2,500 m above sea level (a.s.l.), where cloud belts are formed by ascending moist air masses. They are recognized as "storehouses" of biodiversity since they host relevant concentrations of the world's species biodiversity as well as high rates of endemism (Hamilton et al. 1995; Aldrich et al. 2000). Cayuela et al. (2006) point out that only 2.5% of the total area of the world's tropical forests is specified as "montane cloud forest", but no

accurate data are available about the actual worldwide distribution. Cloud forests belong to the world's most endangered ecosystems as they are affected, for instance, by changes of land use such as the conversion to pasture and croplands (Doumenge et al. 1995; Cayuela et al. 2006). Furthermore, the global warming forces a lifting of the condensation level along with a reduction of fog frequency (Lawton et al. 2001). The raise in cloud base and thus the displacement of the minimum level of montane cloud forests cause considerable ecological changes for the organisms adapted to that habitat (Pounds et al. 1999; Bruijnzeel 2001). Bruijnzeel and Hamilton (2000) even stated that with an increase in global warming montane cloud forests are likely to disappear.

During the last decades, an enhanced interest in montane cloud forest is evident (*e.g.*, Hamilton et al. 1995; Cavelier et al. 1996, 1997; Bruijnzeel and Veneklaas 1998; Clark et al. 1998; Bruijnzeel 2001, 2004; Holder 2003, 2004; Chang et al. 2006; Eugster et al. 2006; Holwerda et al. 2006; Klemm et al. 2006; Leon-Vargas et al. 2006). The ecological significance of montane cloud forests is, among other factors, due to their unique hydrological conditions. The vegetation gathers water from wind-blown fog and thus captures a significant contribution to the hydrological cycle and nutrient budget. The contribution of fog water as an additional water source to the hydrological budget of forest ecosystems is well documented (Zadroga 1981; Hutley et al. 1997; Zimmermann et al. 1999; DeFelice 2002; Liu et al. 2004). The recognition of the ecological value of montane cloud forests led to the establishment of various international initiatives that aim at the implementation of research, conservation and restoration activities (Aldrich 1998; Aldrich et al. 2000; Bubb et al. 2004). However, few studies are available that focus on nutrient input through fog water deposition, since the simultaneous measurements of fogwater deposition and the chemical composition of the fog water sample that represents exactly the same time period are required (*e.g.*, Thalmann et al. 2002). The experimental quantification of occult deposition fluxes is still a challenge in atmospheric research due to its technical instrument requirements and methodological difficulties. Different approaches were applied to quantify the fogwater (occult) deposition such as modeling of fog water deposition fluxes (Lovett 1984) or the estimation of the water deposition by weighing plants (Chang et al. 2002). In this study, we present the results of a 47-day experimental period of direct measurements of fogwater fluxes at a montane cloud forest in Taiwan. The eddy covariance method was applied in combination with an active fogwater collector to examine the deposition fluxes of nutrients into the ecosystem. We compared the nutrient input through occult deposition to the deposition of water and nutrients through wet deposition (rain). To our knowledge, this study presents the only measurements of turbulent fogwater fluxes by using the eddy covariance method available for Southeast Asia.

The quantification of the nutrient input through occult and wet deposition will improve the understanding of the biogeochemical cycle functions in montane cloud forests. In this study, we discuss the concentrations of various ions in fog water versus rainwater and evaluate the role of occult and wet deposition into the ecosystem. The overall scope of this study is to illuminate the influence of fog on the endemic appearance of the respective cypress forest. We presume that fog is the key factor that determines the vegetation structure since fog affects the plants' metabolism. Fog reduces photosynthesis through lowering solar radiation and decreased air temperature, as well as reducing the mineral uptake associated with lower transpiration during foggy conditions (Bruijnzeel and Veneklaas 1998).

2 Experimental

2.1 Site Description

The study took place at the Chilan research site (1,650 m a.s.l.) in north-eastern Taiwan (Chang et al. 2006; Klemm et al. 2006). The predominant tree species of the cloud forest are *Chamaecyparis obtusa* var. *formosana* (yellow cypress) and *Chamaecyparis formosensis* (red cypress). The appearance of both endemic *Chamaecyparis* species is assumed to be strongly coupled with abundant frequency of fog. The fog duration ranges from 4.7 to 11 h per day (Chang et al. 2002). The reduction of incoming shortwave radiation due to fog as well as the constant exposure to acidic fog water deposition account for important ecological aspects for the growth of the endemic cypress forest (Liao et al. 2003).

The measurements were carried out in the partly managed forest beside the nature preserve. The canopy layer is considerably closed and uniform; its average height is 9.8 m. The instruments were mounted on an experimental tower (24°35′27.4″N and 121°29′56.3″E) at 23.4 m (eddy covariance setup) and 20.4 m (fogwater collector) above ground, respectively.

2.2 Methods

2.2.1 Fog Deposition Measurements

The turbulent fogwater fluxes were determined by means of the eddy covariance method (*e.g.*, Stull 1988). This method is often described as the only direct flux measurement technique for fog (Gallagher et al. 1992; Vong and Kowalski 1995; Burkard et al. 2002). The experimental setup consisted of a Young 81000 ultrasonic anemometer (R.M. Young, USA) in combination with a fog droplet spectrometer (model FM-100, Droplet Measurement Technologies, Boulder, USA). The sample frequency was 12.5 Hz and the averaging interval was 30 min. The fog droplet spectrometer detected the number and size of fog droplets by scattering of a laser beam and recorded the spectra of fog droplets with mean diameters from 2 μm to 50 μm within 40 channels.

The turbulent flux F_x of an entity x can be quantified as

$$F_x = \overline{w'x'} \tag{1}$$

where w is the vertical wind speed and x is, for example, the liquid water content. The primes denote the deviation of individual measurements from the mean (*e.g.* 30 min averaging period) and the overbars indicate the time average of the 30 min averaging interval. The wind vector coordinates were double rotated to align the main axis with the streamlines and to yield zero average v and w wind components, respectively.

The gravitational deposition $D_{gravitational}$ was determined after the Stokes' settling velocity v_s (Beswick et al. 1991). The total fogwater flux was calculated by adding the turbulent and the gravitational flux. Positive fogwater fluxes are directed upward and negative fogwater fluxes are directed downward. The extent of atmospheric turbulence was characterized by means of the friction velocity u_*.

2.2.2 Gap Filling

For this study, we used an artificial neural network to fill small data gaps in the fogwater flux time series caused by instrument malfunctions. Artificial neural networks are mathematical modeling tools to cognize and represent arbitrary complex relationships between input and somehow related output values. Due to their ability to learn from given cause-and-effect datasets or ancient time series, artificial neural networks became a useful tool for several problems in the field of statistic, economy and natural sciences (Patterson 1996). The application of artificial neural networks is an approved feature to substitute missing values (Papale and Valentini 2003).

For our purpose, a multi-layer perceptron network (MLP) was trained with available datasets in order to find a mapping rule for the 4-dimensional input values consisting of, in our case, the mean air temperature, incoming shortwave radiation, wind direction, and visibility onto the target value, *i.e.* the measured water deposition fluxes. An MLP network consists of several connected nodes arranged in layers. These nodes or 'neurons' generate simple functions of the received input values. The input of a single neuron is built of a weighted sum of the outputs from all connected neurons in the previous layer. Due to the multiple connections, a network of such neurons can principally model any non-linear function (Bishop 1995; Patterson 1996). This approach bears the advantage that the underlying relationship between the input data and the target values (*i.e.* the results) are not needed to initialize the model parameters in advance. In contrast to other multivariate gap filling procedures, the artificial neural network is able to learn from available training patterns, which is one the most important differences to other linear or non-linear statistical gap filling procedures (Stauch and Jarvis 2006). The iterative learning process within an artificial neural network is realized by changing the weights and thresholds of the neurons which influence the activation values of the neurons in the following layer (Fig. 1). The sum of input values is transformed by a logistic, sigmoid activation function (Bishop 1995) representing the activation value of the neuron which is transmitted to the next layer. The adjustable network parameters were set to reach the lowest error E between the real target values in the training data set and the target

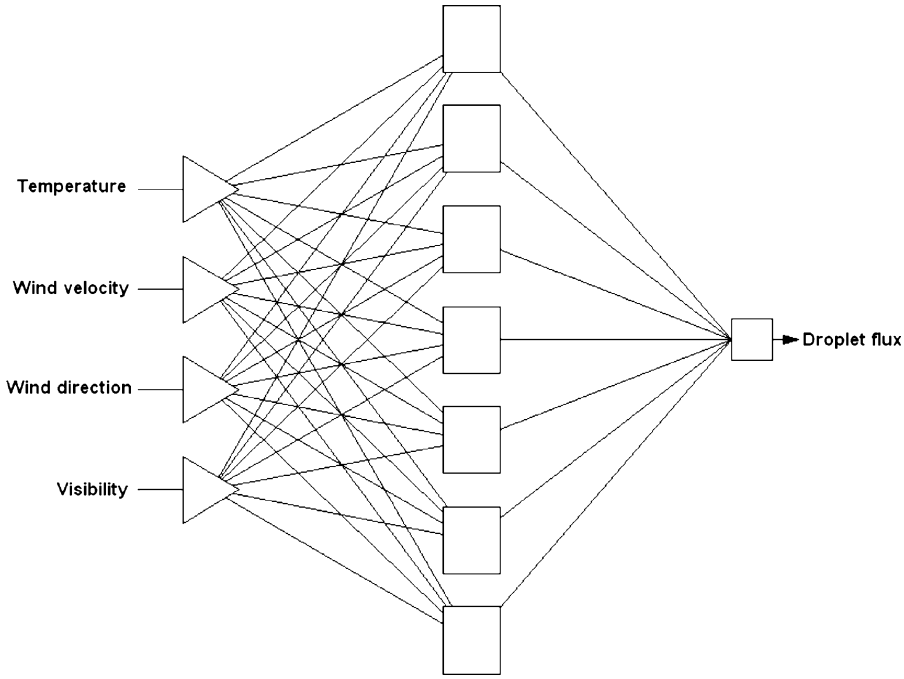

Fig. 1 Schematic diagram of the 4-7-1 layout of the neural network used for the fog water flux reproduction. The neurons belonging to the first input layer transmit the values to the neurons in the second layer. After summation of all inputs in every neuron, the weighted sum is transformed by a logistic function giving the output of the neuron. Thus, the values building the inputs of the third layer's neurons are transformed non-linearly when finally summed and again transformed linearly or nonlinearly in the output layer (see text)

values reproduced by the network. We calculated the mean squared error calculated from all n deviations to obtain the quality of a neural network:

$$E = \frac{1}{n}\sum_{i=1}^{n}(m_i - y_i)^2 \qquad (2)$$

where n is the number of available training datasets consisting of inputs and corresponding target values, m_i are the measured values, and y_i are the output values calculated by the network. During the optimization process, the *quasi-Newton* method (Bishop 1995; Setiono and Hui 1995) was used to find the minimum error function.

2.2.3 Fog and Rainwater Collection

For the fogwater collection, an active strand cloud water collector was used (Wrzesinsky and Klemm 2000). A fan aspirated the foggy air with a consistent velocity of 8.1 m s^{-1}. The fog droplets impacted on the strings (Teflon) due to their inertness and slid along the strings through a tube (Teflon) into an automated sampler (ISCO, USA). The sampling area of the active cloud water collector was 650 cm^2. Whenever the visibility (MIRA visibility sensor 3544, Aanderaa instruments, Norway) dropped below 1,000 m, the fog collector was triggered and operated automatically.

The strings as well as all sampling bottles were pre-cleaned with bi-deionised water. The ISCO sampler contained 24 sampling bottles (Polypropylene) of 1 L volume. For most of the time, a new bottle was triggered every one hour to ensure a high sampling resolution. The fog water collected with the ISCO sampler was filled into two 50 mL sampling bottles (high density polyethylene, HDPE). When the sampling volumes were too little, two (or more) bottles were combined.

The amount of precipitation was quantified by a tipping bucket rain gauge (TIC-1, Takeda, Japan). The rain data and other meteorological data were saved at 10 min averages. The rain water samples were collected using a self-made bulk precipitation gauge (HDPE funnel and bottle). The rain water was sampled on a per event basis. The rain and fogwater samples were treated in the same way. One 50 mL bottle was frozen immediately to inhibit microbial activity; the other aliquot was used for the measurements of pH and electrical conductivity. Additionally, field blanks were taken for the quality control. All used materials that came into contact with the fog and rain water were chemically inert so that contamination of the water can be excluded.

The event based nutrient deposition [mg m^{-2}] was determined by multiplying the total fog (and rain, respectively) water deposition [L m^{-2}] by the mean concentrations of ions measured in the simultaneously collected water sample [mg L^{-1}]. For the quantification of the ion input through occult and wet deposition for a single event, the sample based nutrient input was summed over the respective time period.

2.2.4 Analytical Procedures

Measurements of pH and electrical conductivity were performed on-site, whereas the chemical analysis of NH_4^+, Na^+, K^+, Ca^{2+}, Mg^{2+}, Cl^-, NO_3^-, PO_4^{3-}, SO_4^{2-}, and F^- were performed in the laboratory at the University of Münster, Germany (Table 1). The pH electrode was calibrated before use. To examine the data quality, an ion balance was computed by summing up the equivalent concentrations of anions $c_{eq,i-}$ and cations $c_{eq,i+}$ for all fog and rainwater samples respectively. According to the condition of electric neutrality, the sum of $c_{eq,i-}$ should be equal to that of $c_{eq,i+}$ for each sample:

$$\sum_i c_{eq,i-} = \sum_i c_{eq,i+} \tag{3}$$

Additionally, for each fogwater sample the theoretical electrical conductivity $x_{theoretical}$ [μS cm^{-1}] was calculated by adding the products of the specific conductivities $x_{specific,i}$ [μS cm^{-1}] and the equivalent concentrations $c_{eq,i}$ of the respective ion i [μeq L^{-1}] after

$$x_{theoretical} = \sum_{ions} x_{specific} \cdot c_{eq} \tag{4}$$

2.2.5 Trajectory Calculations

Backward trajectories were calculated to study the advection regime of air masses and the coherency of the origin of air masses and their pollutant concentrations (Klemm et al. 1994; Thalmann et al. 2002; Tago et al. 2006). For every fogwater sample, a backward trajectory was computed using the HYSPLIT model (Draxler and Rolph 2003; Rolph 2003). Each trajectory indicates the path of the respective air mass during the last 120 h at 1 m above surface level before reaching the fogwater collector.

3 Results

3.1 Fog and Rain Water Chemistry

During the experimental period from August 04 through September 20 in 2006, 217 fogwater samples and 20 rain samples were collected. The results of the chemical analysis are presented in Table 2. The data quality was examined by considering the ion balances of the single samples and by a comparison of the measured with the calculated electrical conductivity. The ion balances indicated a very good agreement

Table 1 Methods and used instruments for the chemical analysis of the fog and rain water samples

Parameter	Method	Instrument
Electrical conductivity	Conductivity electrode	LF 315 (WTW, Germany)
pH	pH electrode	pH 323 (WTW, Germany)
NH_4^+	Flow injection analysis	Aquatec Analyzer 5400 (Aquatec, Sweden)
Na^+	Flame photometry	PEP-7 (Jenway, UK)
K^+	Flame photometry	PEP-7 (Jenway, UK)
Mg^{2+}	Atomic absorption spectroscopy	Optima 3000 (Perkin Elmer, USA)
Ca^{2+}	Atomic absorption spectroscopy	Optima 3000 (Perkin Elmer, USA)
Cl^-	Ion chromatography	DX 100 (Dionex, USA)
NO_3^-	Ion chromatography	DX 100 (Dionex, USA)
SO_4^{2-}	Ion chromatography	DX 100 (Dionex, USA)
PO_4^{3-}	Ion chromatography	DX 100 (Dionex, USA)
F^-	Ion chromatography	DX 100 (Dionex, USA)

Table 2 Statistical parameters of electrical conductivity [μS cm^{-1}], pH, and measured ions [μeq L^{-1}] of all fogwater and rainwater samples collected between 4 August and 20 September 2006 at the Chilan site

	Fog (n=217)					Rain (n=20)				
Parameter	Median	Mean	σ	Min	Max	Median	Mean	σ	Min	Max
Conductivity	52	131	198	2	1,102	8	12	10	2	35
pH	4.13	3.61	0.79	2.24	6.11	4.94	4.74	0.53	4.24	6.59
H^+	74.1	244	496	0.8	5754	11.5	18.2	16.3	0.3	57.5
NH_4^+	56.3	235	412	b.d.l.	2469	5.0	13.2	17.3	0.0	59.4
Na^+	13.2	58.6	124	b.d.l.	732	b.d.l.	1.1	2.0	b.d.l.	4.4
K^+	2.6	10.3	19.5	b.d.l.	139	b.d.l.	b.d.l.	0.6	b.d.l.	2.5
Ca^{2+}	10.5	34.1	63.2	3.5	494	4.7	6.0	2.6	3.0	12.5
Mg^{2+}	7.0	18.8	41.3	1.1	457	2.1	2.0	0.6	1.1	3.3
Cl^-	13.7	42.8	69.9	b.d.l.	399	2.8	2.8	1.7	0.7	6.4
NO_3^-	35.5	179	379	0.9	2992	7.7	12.2	11.4	0.8	32.5
PO_4^{3-}	8.9	18.0	19.5	2.4	61.3	b.d.l.	b.d.l.	b.d.l.	b.d.l.	b.d.l.
SO_4^{2-}	103	401	759	1.7	6329	17.6	28.6	26.0	3.2	93.2
F^-	2.6	6.9	13.4	b.d.l.	90.9	1.3	1.3	0.1	b.d.l.	1.4

σ is the standard deviation; b.d.l. means "below detection limit".

between the sum of anions and the sum of cations. The Pearson's correlation test showed a significant correlation on the $p<0.05$ level (r=0.91 for fog water and r=0.83 for rain water). The median ratio of ∑anions/∑cations was 0.97 for fog water and 0.96 for rain water. The agreement between the measured and calculated conductivity was also very high (r=0.87 for fog water and r=0.98 for rain water). The examination of data quality shows that the samples were analyzed with high accuracy.

The study of the backward trajectories indicated that three advection regimes, which were well distinguished from each other, existed at the study site. Therefore, the trajectories were grouped into three classes (Fig. 2). The air masses of class I travelled exclusively over the Pacific Ocean during the last 120 h before reaching the study site (Fig. 2a). The air masses of class II were carried over the Philippines and reached the Chilan site from the south (Fig. 2b). The pathway of the air masses of class III were advected from mainland China which is located north/north-westerly to the study site (Fig. 2c). The classification of the trajectories led to the hypothesis that systematic differences exist between the three classes concerning their chemical composition. The fog water samples were grouped according to their respective trajectory. The examination of the trajectories yielded 102 fogwater samples classified as class I, 20 samples as class II, and 95 as class III. Table 3 shows the statistical parameters of the respective classes.

Statistical tests were applied to examine if the classification of the fogwater samples on the basis of the trajectories was statistically meaningful. A Kolmogorov–Smirnov test confirmed that the pH, electrical conductivity, and all analyzed ions (except for K^+ and Ca^{2+}) were log-normally distributed. By using a Levene's test, the homogeneity of variances was tested. The variances of the data set were homogeneous ($p<0.05$) and thus, a one-way analysis of variance (ANOVA) could be applied to test if the differences between the classes are statistically significant (Table 4). The variances of the classes were significantly different from each other ($p<0.05$). The Tukey test was used to examine which classes were significantly different from each other on the $p<0.05$ level (Table 5). Since K^+ and Ca^{2+} were neither normally distributed nor the homogeneity of variances was given, a non-parametric Kruskal–Wallis ANOVA was applied to test if there are significant differences between the classes (Table 4). Afterwards, a Mann–Whitney test was used (Table 5).

The statistical analysis arrived at the result that the classification of the fogwater samples on the basis of the pathway of the trajectories was plausible. The differences between class I and class III were throughout extremely significant (highly significant for Na^+, respectively) for all analyzed parameters. The differences between class II and class III were extremely significant for SO_4^{2-}, highly significant for electrical conductivity, pH, NH_4^+, and Ca^{2+} as well as

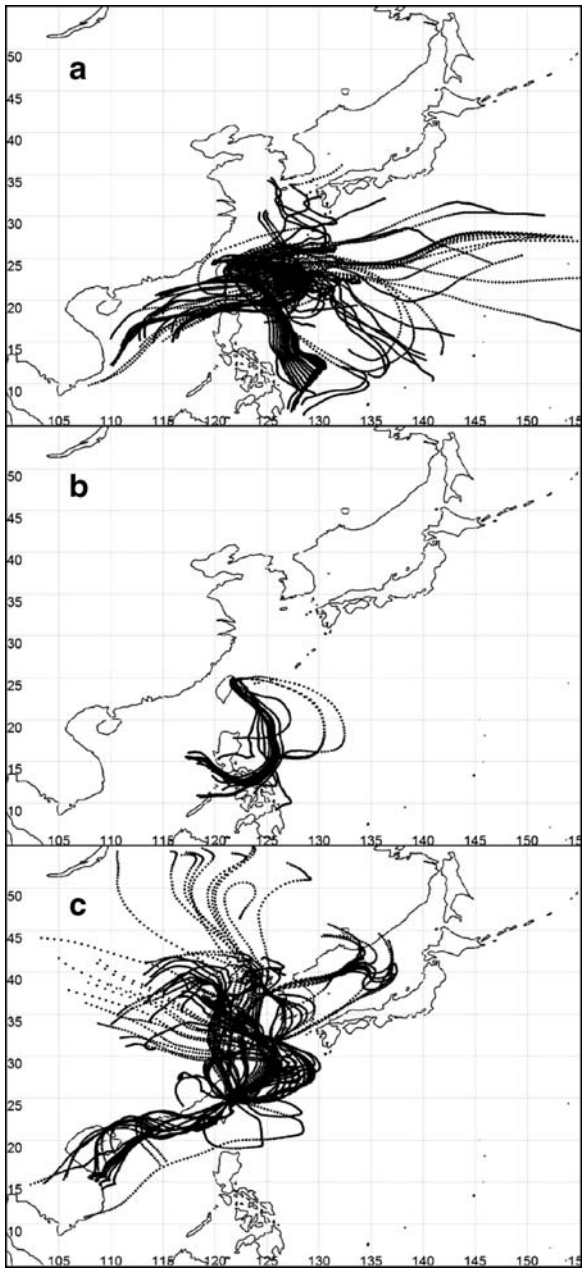

Fig. 2 Backward trajectories representing the last 120 h before reaching the Chilan site (24°35′27.4″N and 121°29′56.3″E). **a**: All trajectories categorized as class I (n=102). **b**: All trajectories categorized as class II (n=20). **c**: All trajectories categorized as class III (n=95)

significant for Mg^{2+}. For Na^+, K^+, Cl^-, and NO_3^-, the differences were not significant. Class I and class II were not significantly different for any analyzed parameter.

The ANOVA did not achieve a result for PO_4^{3-} and F^- since the number of samples of class II was too small due to the low concentrations that ions.

A Kolmogorov–Smirnov test showed that the rainwater samples were log-normally distributed ($p<$ 0.05). A single t-test (for the electrical conductivity, pH, NH_4^+, Na^+, Mg^{2+}, Cl^-, NO_3^-, SO_4^{2-} and F^-) and a non-parametric Mann–Whitney test (for K^+ and Ca^+, because no Gaussian distribution was given for the fog water) was applied to examine the differences between the fog and rain water. The differences were found to be significant for all parameters (except for K^+ and F^-: not significant) on the $p<0.05$ level. For PO_4^{3-}, the t-test was not applied as the concentrations were below detection limit. The total mean equivalent concentration of the fogwater samples was 1,249 μeq L^{-1} and 86 μeq L^{-1} for the rain water samples. Thus, the total mean equivalent concentration was about 15 times higher in the fog than in the rain water.

For both the fog and rainwater samples, H^+, NH_4^+, NO_3^-, and SO_4^{2-} contributed most to the total equivalent concentration. Those ions made up 85% of the total equivalent concentration in the fog water and 84% in the rain water.

3.2 Occult and Wet Deposition

During August 04 through September 20 in 2006, 5.77 mm fog water was deposited into the ecosystem by means of turbulent deposition plus gravitational deposition. In contrast, 1,150 mm were deposited by precipitation (wet deposition) during the same period. The total fogwater fluxes ranged between +31.7 mg m^{-2} s^{-1} (emission fluxes) and −56.6 mg m^{-2} s^{-1} (deposition fluxes). The mean liquid water content (*LWC*) as averaged over periods with fog (visibility< 1,000 m), was 83.9 mg m^{-3}, and the mean total fog water flux was −4.1 mg m^{-2} s^{-1}. We did not find any systematic differences in liquid water content concerning the trajectories or advection regime.

The bimodal pattern of the median normalized droplet number size distribution (Fig. 3) shows mean droplet diameters d with 2 μm<d<6 μm and 9 μm<d <15 μm were the most frequent. Larger fog droplets with mean diameters of 15 μm<d<25 μm contributed most to the total fog water flux. The sedimentation velocity of the fog droplets v_s was calculated. It ranged between 0.007 cm s^{-1} for mean droplet diameters of 1.5 μm and 7.24 cm s^{-1} for mean

Table 3 Median values, averages and standard deviation of the particular advection classes

	Class I (n=102)			Class II (n=20)			Class III (n=95)		
Parameter	Median	Average	σ	Median	Average	σ	Median	Average	σ
Conductivity	26.2	56.5	84.7	79.2	72.1	58.5	119	214	254
PH	4.43	4.03	0.73	3.85	3.91	0.78	3.69	3.37	0.67
H^+	37.2	87.2	136	141	123	108	204	426	690
NH_4^+	28.7	88.8	179	57.3	60.4	57.2	152	398	505
Na^+	8.7	34.4	78.8	8.7	28.1	42.6	26.3	84.5	156
K^+	2.5	3.8	6.0	2.5	3.0	3.9	7.5	18.0	26.2
Ca^{2+}	8.5	20.9	38.4	10.0	11.6	7.0	17.0	49.1	77.7
Mg^{2+}	4.1	10.3	16.4	6.4	9.0	9.0	9.9	28.1	56.9
Cl^-	6.9	24.5	44.7	11.6	29.7	41.5	31.8	62.3	87.1
NO_3^-	23.0	85.6	193	56.1	78.1	75.8	85.6	270	462
PO_4^{3-}	5.5	11.7	15.0	b.d.l.	b.d.l.	b.d.l.	18.2	22.2	19.1
SO_4^{2-}	57.3	122	199	89.5	114	110	316	729	1018
F^-	1.4	7.0	22.4	3.2	3.2	n.d.	5.1	7.1	6.8
∑cations	103			240			455		
∑anions	95			227			442		

Ion concentrations of the fog water are given in unit μeq L^{-1} and electrical conductivity is given in μS cm^{-1}.

droplet diameters of 49 μm. The friction velocity u_* is a measure to characterize the development of the turbulence regime (Foken 2003). For a friction velocity u_*>0.1 m s^{-1}, turbulent conditions were assumed. In 18.7% of the data set, that condition was not fulfilled.

The eddy covariance setup performed as expected, even though small data gaps were inevitable. Large rain droplets caused technical problems and device failures. The experimental site is located in a remote area where the power supply is not permanently guaranteed. In case of heavy thunderstorms, short power failures occasionally occurred. Otherwise, the instrumentation performed very reliably. Since for the calculation of the nutrient input a complete data set of chemical analysis and the respective deposition data are required, small gaps in the data set were filled by the help of a artificial neural network (Section 2.2.2) (Fig. 4). The correlation between the originally measured fogwater flux data and the simulated flux data was examined using the Pearson's correlation test. That test showed a significant correlation (r=0.73) on the p<0.05 level.

3.3 Nutrient Input through Occult and Wet Deposition

The nutrient input through occult and wet deposition was calculated on the basis of 217 fog water and 20 rainwater samples, both completely covered the experimental phase. For the consideration of the sample based input of H^+, NH_4^+, Na^+, K^+, Ca^{2+}, Mg^{2+}, Cl^-, NO_3^-, PO_4^{3-}, SO_4^{2-} and F^-, the quantity of water deposition and the chemical analysis of the respective water sample were regarded. Figures 5 and 6 show the event based nutrient input through occult and

Table 4 Significance of the differences within the group of all fogwater samples tested using a one-way ANOVA (electrical conductivity, pH, NH_4^+, Ca^{2+}, Mg^{2+}, Cl^-, NO_3^-, PO_4^{3-}, SO_4^{2-}, and F^-) and a Kruskal–Wallis ANOVA (K^+ and Ca^{2+})

Parameter	Significance
Conductivity	***
pH	***
H^+	***
NH_4^+	***
Na^+	*
K^+	***
Ca^{2+}	***
Mg^{2+}	***
Cl^-	***
NO_3^-	***
PO_4^{3-}	–
SO_4^{2-}	***
F^-	–

The level of significance was termed after: n.s. – not significant, * – significant (p<0.05), ** – highly significant (p<0.01), ***extremely significant (p<0.001). For PO_4^{3-} and F^-, the ANOVA did not achieve a result due to the limited data set of class II.

Table 5 Differences between the classes (determined on the basis of the trajectories) tested with a Tukey test (electrical conductivity, pH, NH_4^+, Ca^{2+}, Mg^{2+}, Cl^-, NO_3^-, PO_4^{3-}, SO_4^{2-}, and F^-) and a Mann–Whitney test (K^+ and Ca^{2+})

Parameter	Class	Class I	Class II	Class III
Conductivity	Class I	1	n.s.	***
	Class II		1	**
	Class III			1
pH	Class I	1	n.s.	***
	Class II		1	**
	Class III			1
H^+	Class I	1	n.s.	***
	Class II		1	**
	Class III			1
NH_4^+	Class I	1	n.s.	***
	Class II		1	**
	Class III			1
Na^+	Class I	1	n.s.	*
	Class II		1	n.s.
	Class III			1
K^+	Class I	1	n.s.	***
	Class II		1	n.s.
	Class III			1
Ca^{2+}	Class I	1	n.s.	***
	Class II		1	**
	Class III			1
Mg^{2+}	Class I	1	n.s.	***
	Class II		1	*
	Class III			1
Cl^-	Class I	1	n.s.	***
	Class II		1	n.s.
	Class III			1
NO_3^-	Class I	1	n.s.	***
	Class II		1	n.s.
	Class III			1
SO_4^{2-}	Class I	1	n.s.	***
	Class II		1	***
	Class III			1

The level of significance was termed after: n.s. – not significant, * – significant ($p<0.05$), ** – highly significant ($p<0.01$), ***extremely significant ($p<0.001$).

wet deposition. The total nutrient input during the study period is shown in Table 6. The dominating ions were NH_4^+, NO_3^-, and SO_4^{2-} (and Cl^- for wet deposition, respectively). The total input of nitrogen by means of occult deposition was 18 mg m^{-2} (10 mg m^{-2} through NH_4^+ and 8 mg m^{-2} through NO_3^-). The sulfur input was 17 mg m^{-2}. For wet deposition, the input of nitrogen was 167 mg m^{-2} (77 mg m^{-2} through NH_4^+

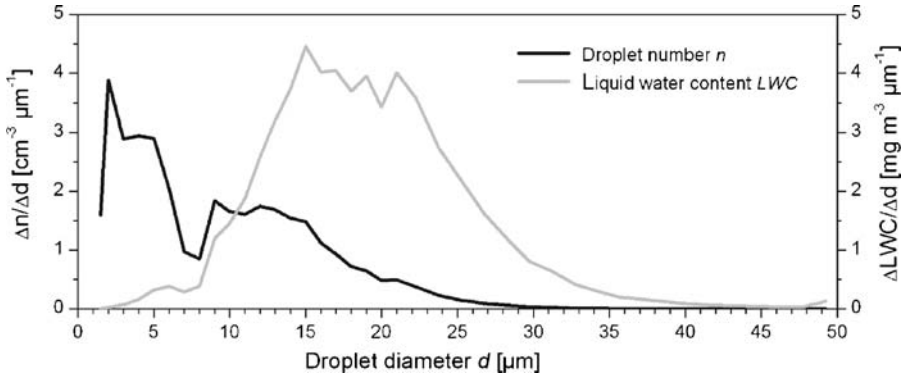

Fig. 3 Median droplet size distribution of droplet number *n* (black line) and liquid water content *LWC* (*grey line*) on the basis of the medians of all 30-min intervals with foggy conditions (visibility<1,000 m) during 4 August 2006 through 20 September 2006 at the Chilan site

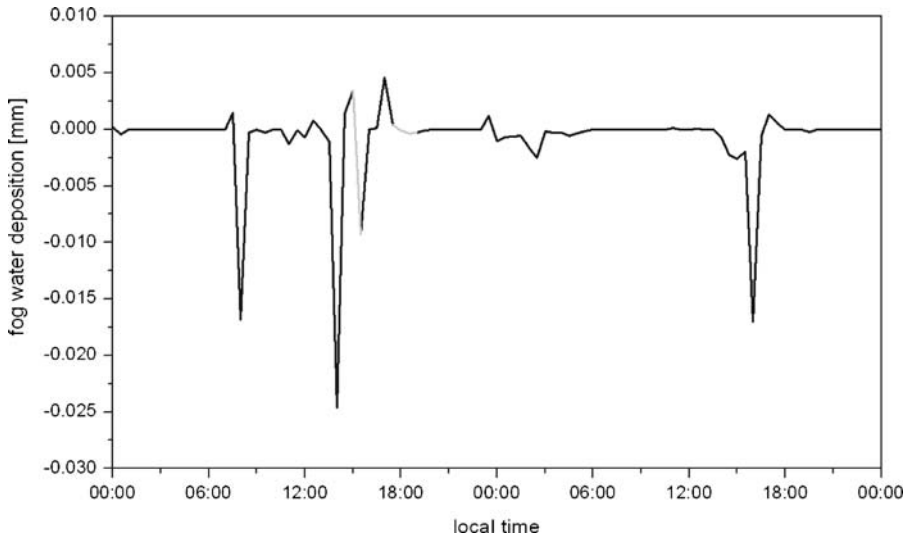

Fig. 4 Pattern of fog water deposition [mm] during 27 August and 28 August 2006 as an instance for gap filling by using a neural network. The *black line* represents the originally measured fog water deposition and the *grey line* is the reproduced fog water deposition

and 90 mg m^{-2} through NO_3^-). The total input of sulphur was 244 mg m^{-2}.

4 Discussion

4.1 Influence of Air Mass History on Chemical Composition of Fog Water

Large differences of ion concentrations were found between the groups of fogwater samples. Statistical tests proved that the classification of the fogwater samples on the basis of the backward trajectories was mostly appropriate and plausible. The differentiation between class I and class III as well as between class II and class III was statistically significant. However, the differences between class I and class II were not significant although the concentrations of ions associated with anthropogenic activity (H^+, NH_4^+, NO_3^-, and SO_4^{2-}) were found to be higher for class II. Thus, it is confirmed that the advection regime of an air mass plays an important role for the chemical concentration of the respective fogwater sample. We interpret these differences in terms of air mass histories of the three classes, and differences of uptake of ions and their precursors during their travel

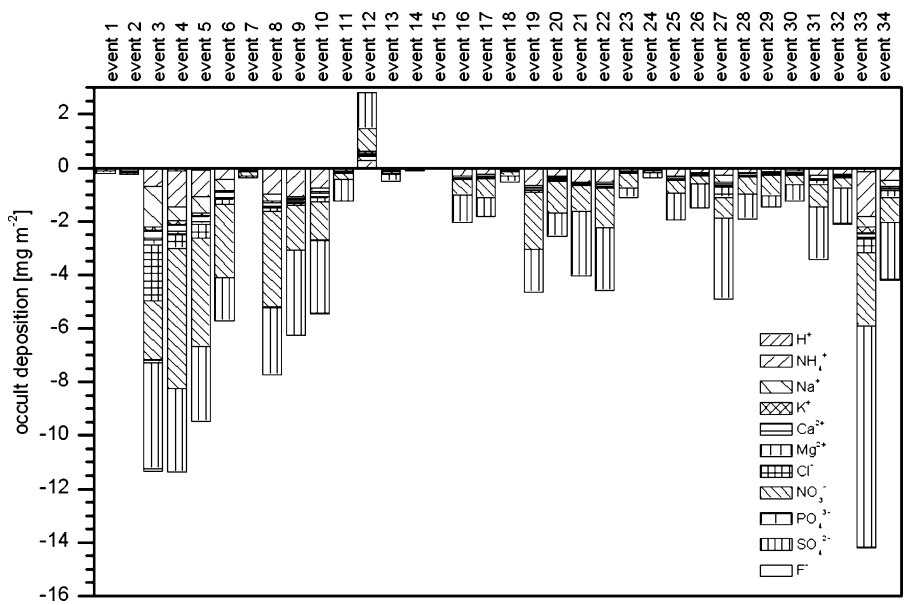

Fig. 5 Nutrient input through occult deposition [mg m^{-2}] subdivided into 34 single fog events. A negative deposition means nutrient input into the ecosystem and positive deposition means emission of nutrients as a result of positive fog water fluxes

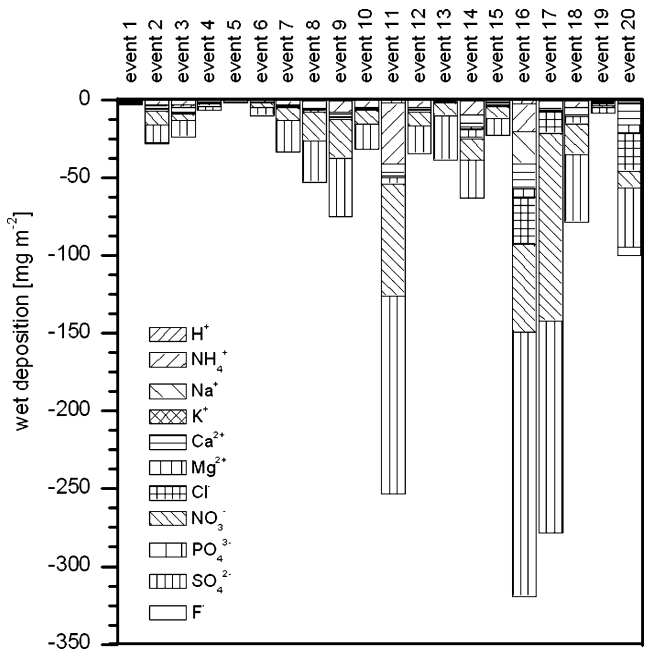

Fig. 6 Nutrient input through wet deposition [mg m^{-2}] subdivided into 20 single rain events

before reaching the sampling site (Klemm et al. 1994; Tago et al. 2006). The base ion charge due to the industrialized region in the western part of Taiwan and the urban agglomeration of the capital Taipei is assumed to be identical for all classes. Air masses classified as class I travel exclusively over the Pacific Ocean and the Taiwan Strait before reaching the study site. Therefore, the fogwater samples of class I exhibit the lowest ion concentrations of ions that are related to anthropogenic activity such as NH_4^+, NO_3^-, and SO_4^{2-}. The maritime impact plays an important role since the concentration of the sea salt related ions Na^+, Cl^-, Mg^{2+}, and Ca^{2+}, are relatively high (although NH_4^+, NO_3^-, and SO_4^{2-} are still higher concentrated) (see also Munger et al. 1989; Gundel et al. 1994). Air masses categorized as class II were advected from the south and passed the Philippines during their last 120 h. The samples of class II exhibit a similar pattern as class I concerning chemical composition so that those air masses are assumed to be principally influenced by the Pacific Ocean. The anthropogenic influence by means of industry plays a minor role since the agriculture (cultivation of sugar cane, rice, corn, and manioc) is predominant on the Philippines. The differences between of chemical composition between class I and class II were found

Table 6 Total nutrient input through occult and wet deposition [mg m^{-2}] measured from 04 August to 20 September 2006 at the Chilan site ("n.d." means no data)

Ion	Occult deposition [mg m^{-2}]	Wet deposition [mg m^{-2}]	Ratio [wet deposition/occult deposition]
H^+	0.8	10.3	13.3
NH_4^+	12.5	98.7	7.9
Na^+	5.0	23.6	4.8
K^+	1.2	1.8	1.5
Ca^{2+}	2.3	77.7	33.1
Mg^{2+}	0.8	19.3	23.7
Cl^-	5.8	96.2	16.5
NO_3^-	36.6	398.9	10.9
PO_4^{3-}	0.2	n.d.	n.d.
SO_4^{2-}	50.2	732.3	14.6
F^-	0.2	5.3	33.4

to be not statistically significant for any parameter. Class III represents air masses that were transported from mainland China. The fogwater samples of class III show high concentrations of ions attributed to anthropogenic activities. Some trajectories pass directly over the heavily industrialized urban agglomerations of Beijing and Shanghai so that the continental influence can clearly be explained. The differences between class I and class III are significant for all analyzed parameters revealing a distinct air mass history of each classes. The statistical analysis showed that class II adopts a mid-position. For most parameters (pH, conductivity, H^+, NH_4^+, Ca^{2+}, Mg^{2+}, SO_4^{2-}) the differences between class II and class III are significant except for Na^+, K^+, Cl^-, and NO_3^- for which the classes do not differ from each other.

The sample number involved a methodological problem since the class II included only 20 fogwater samples (with very low concentrations that were partly below the detection limit), and an analysis of variance did not yield a positive result. Thus, the differences between the classes for F^- and PO_4^{3-} could not be statistically verified.

The pH, electrical conductivity, concentration of NH_4^+ as well as SO_4^{2-} were found to be the most differentiating parameters that express the grade of the continental or anthropogenic influence, respectively. The burning of carbon and fuel oil, traffic, and industrial processes are considered to be the main sources for NH_4^+ and SO_4^{2-} at the Chilan site. The distribution of these four parameters for class I, class II, and class III are plotted in Fig. 7.

4.2 Contribution of Occult and Wet Deposition to Nutrient Input

The differences between the fog and rainwater samples were found to be statistically significant for most analyzed parameters. The mean absolute ion

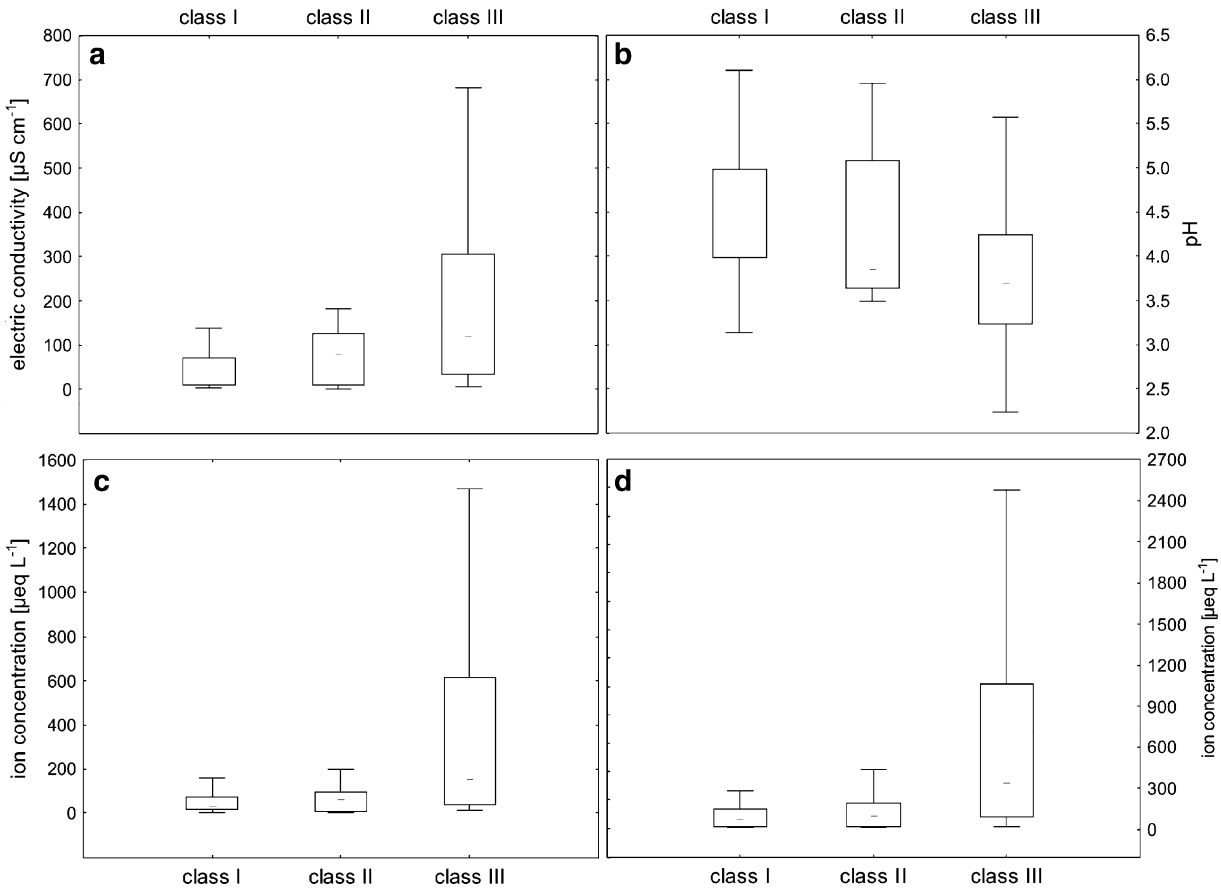

Fig. 7 Box–Whisker plots showing the 5% percentile, 25% percentile, 50% percentile (median), 75% percentile, and the 95% percentile of the electrical conductivity [µS cm^{-1}] (**a**), pH (**b**), the concentration of [µeq L^{-1}] (**c**), and the concentration of [µeq L^{-1}] (**d**) for class I, class II, and class III

concentrations [μeq L^{-1}] were roughly about 5–20 times higher in the fog water than in the rain water. Our results agree well with studies from other experimental sites (Schemenauer et al. 1995; Igawa et al. 1998; Bridges et al. 2002; Beiderwieden et al. 2005). Klemm and Wrzesinsky (2007) report of enrichment factors for NH_4^+, NO_3^-, and SO_4^{2-} in fog versus rain water of 18.1, 12.7, and 11.8, respectively, at a mountainous site in central Europe. The enrichment factors found in our study are 17.8 for NH_4^+, 14.6 for NO_3^-, and 14.0 for SO_4^{2-}, respectively. The differences between fog and rain water may result from the altitude of formation. Fog water represents lower layers of the atmosphere that are more strongly influenced by continental emissions, whereas rain droplets originate at higher altitudes where the atmosphere is less polluted by ground-based emissions (Bridges et al. 2002). Moreover, the rain droplets are much larger and may therefore be more diluted than the fog droplets.

The input of ions through wet deposition has been found to be substantially larger than through occult deposition (Table 6). The ratio between both types of input is as high as 33.4 for F^- and 33.1 for Ca^{2+}. The smallest differences exist for K^+. Geogenic origin and industrial processes are the main sources for potassium, so the concentrations in rain water are relatively low.

Although the ion concentrations of the fog water were notably higher than those of the rain water, the absolute nutrient input originated principally from wet deposition. That discrepancy between the measured ion concentrations and the actual relevance for the ecosystem is solely explained by the net amount of water input. During the experimental period, 5.77 mm water was deposited through fog water, and 1,150 mm were precipitated through rain. Although we measured considerable fogwater deposition, compared to the water input through rain it was of minor significance. The water input through fogwater deposition accounted only for about 0.5% of the total water input during the experimental period. For the Yuan Yang Lake site (about 2 km from the Chilan station), Chang et al. (2002) estimated the fog deposition by exposure experiments with epiphytic bryophytes. They report stand-scale deposition rates of 0.17 mm h^{-1}. This calculates to an estimated daily amount of fog deposition of 4.08 mm. The discrepancy between our measurements and the findings from Chang et al. (2002) may be due to the different characteristics of the respective experimental periods concerning the influencing parameters such as the liquid water content of the foggy air and wind velocity. During the experimental period, the mean wind velocity was very low (<1 m s^{-1} for 57.7% of the time). During 18.7% of the time, the friction velocity u_* was <0.1 m s^{-1} indicating that the turbulence regime was not fully developed. Consequently, the eddy covariance method, measuring the turbulent fog water flux, detected only small fluxes. Especially at night, when atmospheric layering was stabile, the fog water fluxes were very small.

Another reason for the lower fog water depositions measured in this study compared to Chang et al. (2002) may be due to the strong seasonal variation of the occurrence of fog. Chang et al. (2002) found out that during the summer months, the average daily fog duration is 4.7 h while it was 11.0 h during the rest of the year. Since this study was carried out in August and September, we possibly did not measure during a period typical for the entire year. Only during 22.1% of the experimental period, the visibility was <1,000 m (foggy conditions), which corresponds to a daily fog duration of 5.4 h.

During the summer month, typhoons play an important role for the ecosystem and are a major source of rainfall (Chang et al. 2002, 2006). On the 9th August and the 16th September 2006, typhoons fell on the study site and caused heavy precipitation for several days. The measured amount of rainfall of 1,150 mm within 47 days is not representative, either. Depending on number and strength of typhoons, the annual rainfall is highly variable and varies between 2,000 mm and 5,000 mm. In any case, our experimental period was dominated by high precipitation amounts. For May 2003, Chang et al. (2006) report that the contribution of fog reached 35% of the total water input, while in September 2003 the fog/rain ratio reduced to only 5% due to the high precipitation brought by a typhoon.

We consequently suppose that the contribution of fog water to the nutrient input has been overestimated so far. We alternatively assume that the reduction of incoming shortwave solar radiation through fog is the most striking ecological factor influencing the vegetation structure and thereby the growth of the endemic cypress forest. Fog reflects about 90% of incoming short wave radiation (Häckel 1999). The mean daily sunshine duration is drastically reduced during foggy

conditions. As a consequence, the biological activity, or rather the rate of photosynthesis, is diminished. Lai et al. (2005) found out that both *Chamaecyparis* species have their optimal growth rate under medium light conditions from 18 to 24 W m^{-2} photosynthetically active radiation. The occurrence of fog may thus be an advantage for the *Chamaecyparis* species in the inter-specific competition since they are able to perform photosynthesis very effectively even under foggy conditions. Additionally, the fog water itself influences the physiological conditions and may be a stress factor due to the direct and persistent contact of the acidic solution with the plant surface (Paoletti et al. 1989; Kohno et al. 2001).

Our results of the fog and rain chemistry agree very well with the data of ion concentrations given in Chang et al. (2002) for the adjacent measuring station. Compared to other sites, the ion concentrations of the fog water at the Chilan site are relatively low (*e.g.*, Olivier and de Rautenbachn 2002; Burkard et al. 2003). The study site is situated in a rural area. The maritime influence is evident due to the comparatively high concentrations of Na^+ and Cl^-. However, the prevalent weather situation has strong impact on the ion loading and thus, the air chemistry. Advection of air masses from mainland China implies a significant nutrient input for the ecosystem. The contribution of ions attributable to anthropogenic activity, such as NH_4^+, NO_3^-, and SO_4^{2-}, is significantly correlated with the air mass transport from China. The most intensive interrelation between advection and nutrient input exists for SO_4^{2-}. During the experimental period, 31 mg m^{-2} SO_4^{2-} were deposited through occult deposition with air masses originating from China, whereas only 19 mg m^{-2} were deposited during air mass advection from the Philippines and the Pacific Ocean.

Due to the requirement of a complete data set of chemical analysis and the respective deposition data for the calculation of the nutrient input, small gaps in the data set were filled using an artificial neural network. The pattern of the simulated flux data reproduced by the artificial neural networks and of the originally measured flux data conformed well. Hence, the closing of the data gaps with MLP networks by means of the corresponding climate data from a nearby station seems to provide a good approximation for otherwise lost data intervals. Our correlation coefficient of $r=0.73$ expresses a high correlation between the originally measured fog water flux data and the simulated flux data. We consequently conclude that the gap filling by using artificial neural networks was justified.

5 Conclusions

The appearance of both endemic *Chamaecyparis* species is assumed to be deeply coupled with the occurrence of fog. Our results indicate that the pertinence of fog for the forest ecosystem is not due to the relevant nutrient input. The nutrient input through wet deposition exceeded the input through occult deposition by far. During our experimental period of 47 days, we found that the input of nutrients through wet deposition was about 14 times higher than through occult deposition. 93% of total nutrient input originated from rain, and just 7% entered the ecosystem through fogwater deposition. These large differences result from the different magnitudes of water input. The ecosystem gained about 285 times more water input by the means of rain than by fog deposition. The examination of the meteorological conditions shows that our experimental period was characterized by exceptionally high rainfall and relatively low fog frequency. The occurrence of typhoons in the summer months is therefore an important ecological factor for the nutrient budget of the cypress forest, even though the runoff water is assumed to play an important role in the hydrological budget of a typhoon event as well. We conclude that the contribution of fog water to the nutrient budget of the ecosystem has been overestimated so far.

The median pH of all fogwater samples was 4.13, and the events of class III (air masses originating from mainland China) exhibited a median pH of 3.69. During weather situations with advection of air masses from north-northwest, an enhanced nutrient input was observed. The nutrient input was substantially lower during air mass transport from westerly and southerly directions. The chemical composition of the fogwater samples was led back to the origin of the air mass and the subsequent pathway. We conclude that the weather conditions have an influence on the nutrient input through occult deposition into the ecosystem.

Acknowledgements This study was supported by the Deutsche Forschungsgemeinschaft (DFG, Kl623/6). We thank A. Held, N.

Hölzel, and D. Lai for their help in the field and during data analysis. Language-editing by M. Zanetti is gratefully acknowledged. The authors gratefully acknowledge the NOAA Air Resources Laboratory (ARL) for the provision of the HYSPLIT transport and dispersion model and READY website (http://www.arl.noaa.gov./ready.html) used in this publication.

References

Aldrich, M. (1998). *Tropical montane cloud forests. Planning and advisory workshop report*. Cambridge: World Conservation Monitoring Centre.

Aldrich, M., Bubb, P., & Hostettler, S. (2000). *Tropical montane cloud forests. Time for action. Arborvitae*. Gland and Cambridge: WWF International, IUCN.

Beiderwieden, E., Wrzesinsky, T., & Klemm, O. (2005). Chemical characterization of fog and rain collected at the Eastern Andes cordillera. *Hydrology and Earth System Sciences, 9*, 185–191.

Beswick, K. M., Hargreaves, K. J., Gallagher, M. W., Choularton, T. W., & Fowler, D. (1991). Size-resolved measurements of cloud droplet deposition velocity to a forest canopy using an eddy correlation technique. *Quarterly Journal of the Royal Meteorological Society, 117*, 623–645.

Bishop, C. (1995). *Neural networks for pattern recognition*. Oxford: University Press.

Bridges, K. S., Jickjells, T. D., Davies, T. D., Zeman, Z., & Hunova, I. (2002). Aerosol, precipitation and cloud water chemistry on the Czech Krusne Hory plateau adjacent to a heavily industrialised valley. *Atmospheric Environment, 36*, 353–360.

Bruijnzeel, L. A. (2001). Hydrology of tropical montane cloud forests: A reassessment. *Land Use and Water Resources Research, 1*, 1.1–1.18.

Bruijnzeel, L. A. (2004). Hydrological functions of a tropical forest: Not seeing the soil for the trees? *Agriculture, Ecosystems and Environment, 104*, 185–228.

Bruijnzeel, L. A., & Hamilton, L. S. (2000). *Decision time for cloud forests. Humid tropics programme series no 13*. Paris: IHO-UNESCO.

Bruijnzeel, L. A., & Veneklaas, E. J. (1998). Climatic conditions and tropical montane forest productivity: The fog has net lifted yet. *Ecology, 79*, 3–9.

Bubb, P., May, I., Miles, L., & Sayer, J. (2004). *Cloud forest agenda*. Cambridge: UNEP-WCMC Biodiversity Series, 32.

Burkard, R., Bützberger, P., & Eugster, W. (2003). Vertical fogwater flux measurements above an elevated forest canopy at the Lägeren research site, Switzerland. *Atmospheric Environment, 37*, 2979–2990.

Burkard, R., Eugster, W., Wrzesinsky, T., & Klemm, O. (2002). Vertical divergences of fogwater fluxes above a spruce forest. *Atmospheric Research, 64*, 133–145.

Cavelier, J., Jaramillo, M., Solis, D., & de León, D. (1997). Water balance and nutrient inputs in bulk precipitation in tropical montane forest in Panama. *Journal of Hydrology, 193*, 83–96.

Cavelier, J., Solis, D., & Jaramillo, M. A. (1996). Fog interception in montane forests across the Central Cordillera of Panamá. *Journal of Tropical Ecology, 12*, 357–369.

Cayuela, L., Glicher, D. J., & Rey-Benayas, J. M. (2006). The extent, distribution, and fragmentation of vanishing montane cloud forest in the highlands of Chiapas, Mexico. *Biotropica, 38*, 544–554.

Chang, S.-C., Lai, I.-L., & Wu, J.-T. (2002). Estimation of fog water deposition on epiphytic bryophytes in a subtropical mountain cloud forest ecosystem in Northeastern Taiwan. *Atmospheric Research, 64*, 159–167.

Chang, S.-C., Yeh, C.-F., Wu, M.-J., Hsia, Y.-J., & Wu, J.-T. (2006). Quantifying fog water deposition by in situ exposure experiments in a mountainous coniferous forest in Taiwan. *Forest Ecology and Management, 224*, 11–18.

Clark, K. L., Nadkarni, N. M., Schaefer, D., & Gholz, H. L. (1998). Cloud water and precipitation chemistry in a tropical montane forest, Monteverde, Costa Rica. *Atmospheric Environment, 32*, 1595–1603.

DeFelice, T. P. (2002). Physical attributes of some clouds amid a forest ecosystem's trees. *Atmospheric Research, 65*, 17–34.

Doumenge, C., Gilmour, D. A., Ruiz Perez, M., & Blockhus, J. (1995). Tropical montane forests: Conservation status and management issues. In L. S. Hamilton, J. O. Juvik, & F. N. Scatena (Eds.), *Tropical montane cloud forests. Ecological studies* 110. New York: Springer Verlag.

Draxler, R. R., & Rolph, G. D. (2003). HYSPLIT (Hybrid Single Particle Lagrarian Integrated Trajectory) Modell access via NOAA ARL READY Website (http://www.arl.noaa.gov/ready/hysplit4.htm). Silver Spring, MD: NOAA Air Resources Laboratory.

Eugster, W., Burkard, R., Holwerda, F., Scatena, F., & Bruijnzeel, L. A. (2006). Characteristics of cloud and fogwater fluxes in a Puerto Rican elfin cloud forest. *Agricultural and Forest Meteorology*, doi:10.1016/j.agrformet.2006.07.008.

Foken, T. (2003). *Angewandt Meteorologie – Mikrometeorologische Methoden*. Berlin: Springer-Verlag.

Gallagher, M. W., Beswick, K., & Chourlarton, T. W. (1992). Measurements and modelling of cloudwater deposition to moorland and forests. *Environmental Pollution, 75*, 97–107.

Gundel, L. A., Benner, W. H., & Hansen, A. D. A. (1994). Chemical composition of fog water and interstitial aerosol in Berkeley, California. *Atmospheric Environment, 28*, 2715–2725.

Häckel, H. (1999). *Meteorologie*. Stuttgart: Ulmer-Verlag.

Hamilton, L. S., Juvik, J. O., & Scatena, F. N. (1995). The Puerto Rico tropical cloud forest symposium: Introduction and workshop synthesis. In L. S. Hamilton, J. O. Juvik, & F. N. Scatena (Eds.), *Tropical montane cloud forests. Ecological studies* 110. New York: Springer Verlag.

Holder, C. D. (2003). Fog precipitation in the Sierra de las Minas Biosphere Reserve, Guatemala. *Hydrological Processes, 17*, 2001–2010.

Holder, C. D. (2004). Rainfall interception and fog precipitation in a tropical montane cloud forest of Guatemala. *Forest Ecology and Management, 190*, 373–384.

Holwerda, F., Burkard, R., Eugster, W., Scatena, F. N., Meesters, A. G. C. A., & Bruijnzeel, L. A. (2006). Estimating fog deposition at a Puerto Rican elfin forest site: Comparison of the water budget and eddy covariance methods. *Hydrological Processes, 20*, 2669–2692.

Hutley, L. B., Doley, D., Yates, D. J., & Boonsaner, A. (1997). Water balance of an Australian subtropical rainforest at altitude: The ecological and physiological significance of

intercepted cloud and fog. *Australian Journal of Botany, 45*, 311–329.

Igawa, M., Tsutsumi, T. M., & Hiroshi, O. (1998). Fogwater chemistry at a mountainside forest and the estimation of the air pollutant deposition via fog droplets based on the atmospheric quality at the mountain base. *Environmental Science & Technology, 36*, 1–6.

Klemm, O., Bachmeier, A. S., Talbot, R. W., & Klemm, K. I. (1994). Fog chemistry at the New England Coast: Influence of air mass history. *Atmospheric Environment, 28*, 1181–1188.

Klemm, O., Chang, S. C., & Hsia, Y. J. (2006). Energy fluxes at a subtropical mountain cloud forest. *Forest Ecology and Management, 224*, 5–10.

Klemm, O., & Wrzesinsky, T. (2007). Fog deposition fluxes of water and ions to a mountainous site in Central Europe. Accepted for publication in *Tellus*.

Kohno, Y., Matsuki, R., Nomura, S., Mitsunari, K., & Nakao, M. (2001). Neutralization of acid fog droplets on plant leaf surfaces. *Water, Air, and Soil Pollution, 130*, 977–982.

Lai, I. L., Scharr, H., Chavarria-Krauser, A., Wu, J. T., Schurr, U., & Walter, A. (2005). Leaf growth dynamics of two congener gymnosperm species reflect the heterogeneity of light intensities given in their natural ecological niche. *Plant Cell and Environment, 28*, 1496–1505.

Lawton, R. O., Nair, U. S., Pielke, R. A., & Welch, R. M. (2001). Climatic impact of tropical lowland deforestation on nearby montane cloud forests. *Science, 294*, 584–587.

León-Vargas, Y., Engwald, S., & Proctor, M. C. F. (2006). Microclimate, light adaption and desiccation tolerance of epiphytic bryophytes in two Venezuelan cloud forests. *Journal of Biogeography, 33*, 901–913.

Liao, C.-C., Chou, C. H., & Wu, J. T. (2003). Regeneration patterns of yellow cypress on down logs in mixed coniferous-broadleaf forest of Yuanyuang Lake Nature Preserve, Taiwan. *Botanical Bulletin of Academia Sinica, 44*, 229–238.

Liu, W. J., Meng, F. R., Zhang, Y. P., Liu, Y. H., & Li, H. M. (2004). Water input from fog drip in the tropical seasonal rain forest of Xishuangbanna, South-West China. *Journal of Tropical Ecology, 20*, 517–524.

Lovett, G. M. (1984). Rates and mechanisms of cloud water deposition to a subalpine Balsam Fir forest. *Atmospheric Environment, 18*, 361–371.

Munger, J. W., Colett, J., Daube, B., & Hoffmann, M. R. (1989). Chemical composition of coastal stratus clouds – dependence on droplet size and distance from the coast. *Atmospheric Environment, 23*, 2305–2320.

Olivier, J., & de Rautenbachn, C. J. (2002). The implementation of fogwater collection systems in South Africa. *Atmospheric Research, 64*, 227–238.

Paoletti, E., Gellini, R., & Barbolani, E. (1989). Effects of acid fog and detergents on foliar leaching of cations. *Water, Air, and Soil Pollution, 45*, 49–61.

Papale, D., & Valentini, R. (2003). A new assessment of European forest carbon exchanges by eddy fluxes and artificial neural network spatialization. *Global Change Biology, 9*, 525–535.

Patterson, D. (1996). *Artificial neural networks*. Singapore: Prentice Hall.

Pounds, J. A., Fogden, M. P. A., & Campbell, J. H. (1999). Biological response to climate change on a tropical mountain. *Nature, 398*, 611–615.

Rolph, G. D. (2003). Real-time Environmental Applications and Display sYstem (READY) Website (http://www.arl.noaa.gov/ready/hysplit4.html). Silver Spring, MD: NOAA Air Resources Laboratory.

Schemenauer, R. S., Banic, C. M., & Urquizo, N. (1995). High elevation fog and precipitation chemistry in Southern Quebec, Canada. *Atmospheric Environment, 29*, 2235–2252.

Setiono, R., & Hui, L. C. K. (1995). Use of a quasi-Newton method in a feedforward neural network construction algorithm. *IEEE Transactions on Neural Networks*, 273–277.

Stadtmüller, T. (1987). *Cloud forests in the humid tropics*. The United Nations University, Tokyo and Centro Agronomico Tropical de Investigacion y Ensenanza, Turrialba, Costa Rica.

Stauch, V., & Jarvis, J. (2006). A semi-parametric gap-filling model for eddy covariance CO_2 flux time series data. *Global Change Biology, 12*, 1707–1716.

Stull, R. B. (1988). *An introduction to boundary layer meteorology*. Dordrecht: Kluwer Academic Press.

Tago, H., Kimura, H., Kozawa, K., & Fujie, K. (2006). Long-term observation of fogwater composition at two mountainous sites in Gunma Prefecture, Japan. *Water, Air, and Soil Pollution, 175*, 375–391.

Thalmann, E., Burkard, R., Wrzesinsky, T., Eugster, W., & Klemm, O. (2002). Ion fluxes from fog and rain to an agricultural and a forest ecosystem in Europe. *Atmospheric Research, 64*, 147–158.

Vong, R. J., & Kowalski, A. S. (1995). Eddy correlation measurements if size-dependent cloud droplet turbulent fluxes to complex terrain. *Tellus, 47 B*, 331–352.

Wrzesinsky, T., & Klemm, O. (2000). Summertime fog chemistry at a mountainous site in Central Europe. *Atmospheric Environment, 34*, 1487–1496.

Zadroga, F. (1981). The hydrological importance of a montane cloud forest area of Costa Rica. In R. Lal & E. W. Russel (Eds.), *Tropical agricultural hydrology*. New York: John Wiley and Sons.

Zimmermann, L., Frühauf, C., & Bernhofer, C. (1999). The role of interception in the water budget of spruce stands in the Eastern Ore Mountains/Germany. *Physics and Chemistry of the Earth, 24*, 809–812.